PHYSICAL REVIEW B VOLUME 19, NUMBER 2 15 JANUARY 1979

Interfacial polarization effects in ionic conductors

M. E. Lines
Bell Laboratories, Murray Hill, New Jersey 07974
(Received 14 September 1978)

The frequency-dependent dielectric response of a simple model ionic conductor has been calculated using boundary conditions that prevent the passage of itinerant ions to or from the sample. The calculation includes the important effects of local fields which lead to an inductive in-phase response in the absence of blocking, and describes the development of interfacial polarization as the applied frequency is decreased. The work allows for the definition of several characteristic frequencies at which the nature of the response changes, including an inductive to capacitive transition in in-phase response at higher values of conductivity. These features enable a separation of vibrational (intrawell) and hopping (interwell) contributions to be made and also make possible an evaluation of the concentration of conducting ions and an estimate of their relaxation times. A brief application of the results using published data for Ag_4RbI_5, Li_4SiO_4, and vitreous $LiNbO_3$ is also included.

I. INTRODUCTION

In an earlier paper,[1] hereafter referred to as I, the effects of electric-dipole-induced local fields on the dielectric response of ionic conductors were discussed for the case of an infinite sample or of a finite sample with Ohmic contacts, through which the itinerant ions can pass freely into and out from the material. Two major effects were deduced, the first being an enhancement of the low-frequency ionic conductivity over the equivalent situation in the absence of local-field effects and the second the development of a negative (or inductive) contribution to the real part of the dielectric constant. The latter is proportional to the ionic conductivity and can dominate the in-phase response component at moderate carrier concentrations.

The inductive contribution to the dielectric constant seems already to have been observed in a number of instances.[2-5] However, experimentally it is extremely difficult to approximate with accuracy the Ohmic-contact condition so that the earlier findings are usually masked experimentally at lower frequencies by contact blocking effects. In this paper we shall consider the opposite extreme from I, namely, the presence of completely blocking contacts through which no itinerant ions can escape or enter the material. This limit is much more closely realizable in practice. We investigate in particular the effects of electric dipolar fields on mobility and diffusion and deduce simple relations describing the development of interfacial polarization with decreasing frequency, and the frequency dependence of the measured dielectric response in the blocking frequency regions. These blocking characteristics usually enable us to separate the vibrational (intrawell) and hopping (interwell) contributions to response and also allow for an independent estimate to be made of the relevant concentration of mobile ions and of their relaxation times. All this information can be extracted from dielectric measurements at frequencies of order of or below the megahertz range.

In this paper we again use the basic model for ionic conductivity set out in I. We consider an assembly of cells (or potential wells) with parallel orientation each of well depth V_M and of spatial extent $2x_M$ (see Fig. 1 of I). A fraction $1-c$ of the sites are considered filled, reducing, in a mean-field approximation, the hopping probability

$$W = c\nu \exp(-V_M/kT) \tag{1.1}$$

by a factor of c from the value $\nu \exp(-V_M/kT)$ that it would have if the adjacent hopping sites were always available (i.e., empty). The frequency ν is termed the attempt frequency and is expected to assume values $10^{12}-10^{13}$ Hz typical of optical phonons although, for reasons not yet wholly understood,[6] values up to several orders of magnitude smaller are often found.

We assume the barrier height V_M to be large compared with kT (thermal energies) so that the physical system represented by the model has two characteristic frequency regions, one associated with intracell motion (which we term vibrational) and one with ion hopping, which are well separated. This being the case, the two responses can be directly summed with little error accruing from interference effects. Paper I investigated the effects of local electric dipolar fields on the hopping and vibrational dielectric response functions ϵ_h and ϵ_v of the system, the total dielectric function ϵ being $1+\epsilon_h+\epsilon_v$. The long-range electrostatic forces cause the effective field $E(\omega)$ at a particular cell site to be shifted in both magnitude and phase from the applied, or Maxwell, field $E_0(\omega)=E_0\exp(-i\omega t)$ at that same site. The form of this shift, if the intracell motion is expressed in a damped-harmonic-

oscillator formalism, is given by Eq. (16) of I as

$$\frac{E(\omega)}{E_0(\omega)} = \frac{\Omega_s^2 - \omega^2 - i\Gamma\omega}{\Omega^2 - \omega^2 - i\Gamma\omega}\,, \tag{1.2}$$

where Γ is the positive damping parameter, Ω_s is the frequency of the in-cell motion in the absence of dipolar forces, and Ω is the (long-wavelength) frequency in the presence of these forces. The magnitude of these shifts depends on the degree to which the itinerant cations (assumed univalent with charge $+e$) are coupled to lattice modes of high optical-mode strength during their in-cell motion. Theoretically, at least, one can even consider the limit of a dielectric instability produced by the dipole forces. The latter situation may actually obtain in amorphous $LiNbO_3$.[7,8]

The final product of I was therefore a series of four equations [Eqs. (24)–(27) of that paper] relating the real and imaginary parts of ϵ_h and ϵ_v to the fundamental microscopic parameters of the problem. Conductivity σ_i $(i = v, h)$ is related to the imaginary response components ϵ_i'', where $\epsilon_i = \epsilon_i' + i\epsilon_i''$, by the equation

$$\sigma_i = \omega\epsilon_i''/4\pi\,. \tag{1.3}$$

For the overdamped case we can introduce the characteristic times $\tau = \Gamma/\Omega^2$ and $\tau_s = \Gamma/\Omega_s^2$ in terms of which the relevant equations become

$$\epsilon_h'(\omega) = -4\pi A_h(\tau - \tau_s)\tau/V(1+\omega^2\tau^2)\tau_s\,, \tag{1.4}$$

$$\sigma_h(\omega) = A_h(1+\omega^2\tau\tau_s)\tau/V(1+\omega^2\tau^2)\tau_s\,, \tag{1.5}$$

$$\epsilon_v'(\omega) = 4\pi\chi_v(0)/V(1+\omega^2\tau^2)\,, \tag{1.6}$$

$$\sigma_v(\omega) = \omega^2\tau\chi_v(0)/V(1+\omega^2\tau^2)\,, \tag{1.7}$$

in which V is cell volume, $\chi_v(0)$ is the static dielectric susceptibility in the absence of hopping, and

$$A_h = 4S^2x_M^2(1-c)W/\lambda kT\,, \tag{1.8}$$

where S is an effective charge parameter and λ is a number which relates the collective mode amplitude x_M to the equivalent itinerant ion amplitude a in that mode according to

$$Sx_M = \lambda ae\,. \tag{1.9}$$

For $\omega\tau \ll 1$, which is typically $\omega \ll 10^9$ sec^{-1}, we note that $\sigma_v(\omega) \to 0$ while $\sigma_h(\omega)$, $\epsilon_v'(\omega)$, and $\epsilon_h'(\omega)$ rapidly approach their static values σ_h [i.e., equal to $\sigma_h(0)$], ϵ_v' and ϵ_h', the true limiting material dielectric parameters. The last of these is related to the conductivity $\sigma = \sigma_h$ in the static limit by

$$\epsilon_h' = -4\pi\sigma(\tau - \tau_s)\,, \tag{1.10}$$

and is always inductive.

With Ohmic contacts, dielectric experiments at frequencies below material dispersion provide only values for σ and $\epsilon' = 1 + \epsilon_v' + \epsilon_h'$. We shall demonstrate below that equivalent measurements with blocking electrodes enable us not only to separate ϵ_v' and ϵ_h' but also to evaluate the concentration parameter c and the relaxation time τ. Blocking effects normally begin at frequencies below material dispersion so that in the blocking equations to be developed we shall neglect the effects of material dispersion, i.e., we assume $\omega\tau \ll 1$ throughout.

II. MOBILITY AND DIFFUSION COEFFICIENTS

The equation of detailed balance including the effects of diffusion and motion under the influence of an applied (Maxwell) field E_0 at lattice coordinate position x is[9,10]

$$\frac{\partial p(x,t)}{\partial t} = D\frac{\partial^2 p}{\partial x^2} - \mu\frac{\partial(pE_0)}{\partial x}\,, \tag{2.1}$$

in which D and μ are the diffusion and mobility coefficients, respectively, and p is the concentration of positive ion carriers per unit volume at the position x at time t. This concentration p, in the presence of the perturbing field E_0, now differs in general from the uniform concentration $p_0 = (1-c)/V$ of negative charge residing in the lattice framework and providing the overall charge neutrality. In this section we determine D and μ as functions of the complex hopping response ϵ_h to which they are obviously physically closely related.

Using the terminology of I, if $\langle n_j\rangle$ is the occupational probability of cell j at time t then in a *local* field $E(\omega)$ the mean field rate equation for hopping to sites $j \pm 1$ is

$$\frac{d\langle n_{j\pm1}\rangle}{dt} = W^{\pm}\langle n_j\rangle\,, \tag{2.2}$$

where[1]

$$W^{\pm} = W[1 \pm (Sx_M/kT)E(\omega)]\,. \tag{2.3}$$

In dynamic equilibrium it follows that a charge

$$q = \frac{d\langle n_{j+1}\rangle}{dt} - \frac{d\langle n_{j-1}\rangle}{dt}\,, \tag{2.4}$$

is effectively transported through a distance $2a$ by this field in 1 sec. The implied current is therefore $j = 2aq$ from which the mobility μ is defined by the relationship

$$j = \mu\langle n_j\rangle E_0(\omega)\,, \tag{2.5}$$

in which $E_0(\omega)$ is the *applied* field. Using (2.2) to (2.5) we obtain the form

$$\mu = (4Wax_MS/kT)[E(\omega)/E_0(\omega)]\,, \tag{2.6}$$

which, in the absence of local-field effects, would be real and frequency independent. The same is true of the diffusivity parameter D which is obtain-

able from (2.6) by use of the Einstein relation

$$\mu/D = e/kT, \tag{2.7}$$

where e is the charge on the carrier (assumed monovalent). From (2.6) and (2.7) we find

$$D = (4Wax_M S/e)[E(\omega)/E_0(\omega)]. \tag{2.8}$$

However, in the presence of local effects μ and D assume frequency-dependent complex values. Using the low-frequency form of (1.2), viz,

$$E(\omega)/E_0(\omega) = (1 - i\omega\tau_s)\tau/(1 - i\omega\tau)\tau_s, \tag{2.9}$$

the mobility (2.6) transforms to

$$\mu = -4i\epsilon_h Wax_M SV\omega/4\pi kTA_h, \tag{2.10}$$

where we have used Eqs. (1.4) and (1.5). Now using Eqs. (1.8) and (1.9) this reduces directly to

$$\mu = -i\omega e\epsilon_h/kTf, \tag{2.11}$$

in which

$$f = 4\pi e^2 p_0/kT. \tag{2.12}$$

From the Einstein relation (2.7) the diffusivity parameter follows as

$$D = -i\omega\epsilon_h/f. \tag{2.13}$$

III. BLOCKING RESPONSE

We now consider Eq. (2.1) subject to a boundary condition for which no mobile cations are allowed to cross the boundary layers at $x = 0, L$, i.e., subject to the restriction

$$\mu p E_0 = D\frac{dp}{dx}, \quad x = 0, L. \tag{3.1}$$

The voltage $V(t)$ between the electrodes is

$$V(t) = \int_0^L E_0(x, t)\,dx. \tag{3.2}$$

Introducing a small probing voltage $V(t) = V_1 \exp(-i\omega t)$ the Maxwell field E_0 and mobile ion concentration p respond in a linear response approximation in the form

$$p(x, t) = p_0 + p_1(x)e^{-i\omega t}, \tag{3.3}$$

and

$$E_0(x, t) = E_1(x)e^{-i\omega t}, \tag{3.4}$$

in which p_1 and E_1 are small quantities.

Using the Poisson equation[11]

$$\frac{\partial E_0}{\partial x} = \left(\frac{4\pi e}{\epsilon_v}\right)(p - p_0), \tag{3.5}$$

together with (3.3) and (3.4), the Eq. (2.1) now linearizes in the form

$$D\frac{d^2 p_1}{dx^2} = \left(-i\omega + \frac{4\pi e\mu p_0}{\epsilon_v}\right)p_1. \tag{3.6}$$

Using the Einstein relation and the definition (2.12) of parameter f this transforms to

$$\frac{d^2 p_1}{dx^2} = \rho^2 p_1, \tag{3.7}$$

where

$$\rho^2 = f/\epsilon_v - i(\omega/D). \tag{3.8}$$

The current density is the sum of displacive and convective contributions in general but, by virtue of the boundary condition (3.1), the latter vanishes at $x = 0, L$. It follows that the total current $J_1 \exp(-i\omega t)$ flowing into and out from the sample per unit area is simply the displacive term at the boundaries, i.e.,

$$J_1 = \left(\frac{\epsilon_v}{4\pi}\right)\left|\frac{\partial E_0}{\partial t}\right|_{x=0} = -\frac{i\omega e_v E_1(0)}{4\pi}. \tag{3.9}$$

The physically relevant (odd symmetry) solution of (3.7) is

$$p_1(x) = A\sinh[\rho(x - \tfrac{1}{2}L)], \tag{3.10}$$

where A is an amplitude parameter that may be determined as a function of applied voltage by integrating (3.5) directly for the Maxwell field and substitution in (3.2). We find

$$\frac{V_1}{A} = \frac{8\pi e}{\epsilon_v \rho^2}\sinh\left(\frac{\rho L}{2}\right) + \left(\frac{D\rho}{\mu p_0} - \frac{4\pi e}{\epsilon_v \rho}\right)L\cosh\left(\frac{\rho L}{2}\right). \tag{3.11}$$

Using Eq. (3.1) to obtain the boundary field

$$E_1(0) = (D\rho A/\mu p_0)\cosh(\tfrac{1}{2}\rho L), \tag{3.12}$$

the current J_1 can now be evaluated in explicit form from (3.9) as

$$J_1 = -(i\epsilon_v \omega e\rho A/f)\cosh(\tfrac{1}{2}\rho L). \tag{3.13}$$

Equation (3.11) and (3.13) can now be combined to provide the formula for admittance Y; it is

$$Y = \frac{A_0 J_1}{V_1} = \frac{-i\epsilon_v \omega A_0}{4\pi}\left(\frac{\omega\epsilon_v + ifD}{\omega\epsilon_v L + (2ifD/\rho)\tanh(\tfrac{1}{2}\rho L)}\right), \tag{3.14}$$

in which A_0 is the electrode area. Expressing the diffusion coefficient in terms of hopping response via Eq. (2.13) now provides the final form

$$Y = \frac{-i\epsilon_v \omega A_0}{4\pi}\left(\frac{\epsilon_v + \epsilon_h}{\epsilon_v L + (2\epsilon_h/\rho)\tanh(\tfrac{1}{2}\rho L)}\right). \tag{3.15}$$

From this expression the capacitance C and resistance R of the blocking electrode configuration follow from $Y = R^{-1} - i\omega C$ and the blocking values of conductivity σ_B and dielectric constant ϵ'_B from

$$\sigma_B = L/RA_0, \quad \epsilon'_B = 4\pi LC/A_0 . \tag{3.16}$$

The last step in expressing σ_B and ϵ'_B wholly in terms of the material response ϵ_v and ϵ_h obtains by noting from (3.8) and (2.13) that

$$\rho^2 = f(\epsilon_v^{-1} + \epsilon_h^{-1}) . \tag{3.17}$$

Introducing $e_i = e'_i - ie''_i = 1/\epsilon_i$ $(i = v, h)$ we can then express ρ as

$$\rho = [f(e'_v + e'_h)]^{1/2} (1+\alpha^2)^{1/4} [\cos(\tfrac{1}{2}\theta) - i \sin(\tfrac{1}{2}\theta)] , \tag{3.18}$$

in which

$$\alpha = \tan\theta = (e''_v + e''_h)/(e'_v + e'_h) . \tag{3.19}$$

In most circumstances of experimental significance ρL is very large compared with unity. We shall suppose this to be true for this paper, in which case the $\tanh(\frac{1}{2}\rho L)$ factor in the denominator of Eq. (3.15) can be replaced by unity. At higher frequencies for which blocking effects are negligible the Maxwell field is essentially V_1/L throughout the sample. As the applied frequency decreases an interfacial charge distribution develops in boundary layers of width δ, with $\delta/L \sim 1/\rho L \ll 1$, at the electrodes. This layer progressively screens the bulk material and causes the Maxwell field in the bulk volume to decrease with decreasing frequency until it approaches zero (complete screening) at $\omega = 0$. However, throughout this process the bulk material experiences a Maxwell field that is essentially independent of x except within the boundary layers themselves.

In addition, the interfacial charge buildup in the surface layers induces equal and opposite charges in the electrodes, which effectively cancel any local-field contributions inside the bulk from the blocked hopping mechanism. It follows that the two basic assumptions leading to the derivation of Eqs. (1.4) to (1.7) from I—namely, that the effective field is uniform and contains no contribution from the ionic conductivity mechanism itself—remain valid in the blocking electrode context except within the narrow boundary layers themselves. Thus, as long as $\rho L \gg 1$ the present theory should be adequate, except perhaps for resistive terms at extremely low frequencies for which the complete screening limit is approached and for which the entire dielectric response takes place within the boundary layers themselves.

IV. ANALYSIS

The solutions (3.16) for blocking responses σ_B and ϵ'_B, which follow from the admittance formula (3.15), can be analyzed in all their essential features without recourse to numerical computation. For simplicity we shall take $\tau \gg \tau_s$, implying a fairly soft dielectric, and shall assume that $\omega\tau \ll 1$ at all frequencies for which blocking effects are significant. The former condition leads, from (1.4) and (1.5) to the relationship

$$\epsilon'_h = -\omega\tau\epsilon''_h , \tag{4.1}$$

and has been found to hold in Ag_4RbI_5, for example,[2] at frequencies above blocking.

The basic equation to be considered is (3.15) in the limit of ρL finite but large compared with unity, i.e.,

$$4\pi LY = -i\epsilon_v \omega A_0 \rho L(\epsilon_v + \epsilon_h)/(\rho L\epsilon_v + 2\epsilon_h) . \tag{4.2}$$

At the lowest frequencies $\epsilon''_h = 4\pi\sigma/\omega$ dominates the denominator. However, as the frequency ω rises terms in $\rho L\epsilon_v$ become competitive and eventually dominate. In the latter regime we see immediately from (4.2) that

$$4\pi LY = -i\omega A_0(\epsilon_v + \epsilon_h) , \tag{4.3}$$

leading via (3.16) to

$$\sigma_B = (\omega/4\pi)(\epsilon''_v + \epsilon''_h) \tag{4.4}$$

and

$$\epsilon'_B = \epsilon'_v + \epsilon'_h , \tag{4.5}$$

which are measures of the true material properties as set out in I.

At the lowest frequencies $\omega \ll \omega_1$, where

$$\omega_1 = 8\pi\sigma/(f^{1/2} L \epsilon_v'^{1/2}) , \tag{4.6}$$

the capacitance saturates to give a frequency independent "fully blocked" dielectric constant

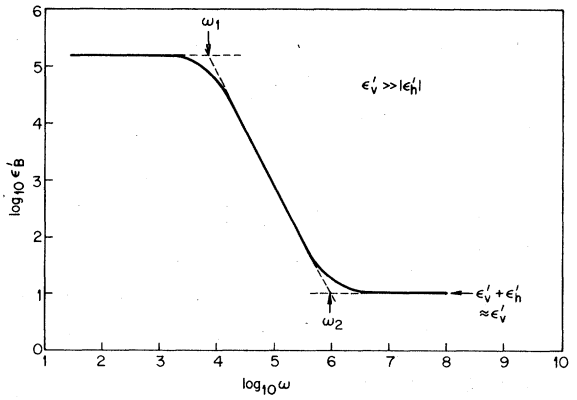

FIG. 1. Blocked dielectric constant ϵ'_B computed numerically from Eq. (3.15) as a function of angular frequency ω for material parameters $\tau = 10^{-10}$ sec, $f^{1/2}L = 10^5$, $\sigma = 10^{-4}$ $(\Omega\,\mathrm{cm})^{-1}$, and $\epsilon'_v = 10$. Since $|\epsilon'_h|$ follows as $4\pi\sigma\tau \approx 0.11$ this represents a dominantly capacitive material response $\epsilon'_v \gg |\epsilon'_h|$. Marked frequencies ω_1 and ω_2 are described in the text.

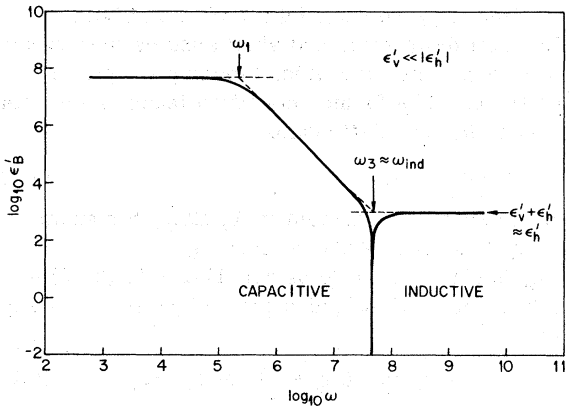

FIG. 2. As Fig. 1 but for material parameters $\tau = 10^{-10}$ sec, $f^{1/2}L = 10^7$, $\sigma = 1\ (\Omega\ \text{cm})^{-1}$, and $\epsilon_v' = 100$. Since $|\epsilon_h'|$ follows as $4\pi\sigma\tau \approx 1.1 \times 10^3$ this represents a dominantly inductive material response $\epsilon_v' \ll |\epsilon_h'|$. The region marked capacitive corresponds to a positive value of response ϵ_B' and that marked inductive to a negative value of this response. Marked frequencies ω_1, ω_3 and ω_{ind} are discussed in the text.

$$\epsilon_B' = \tfrac{1}{2} f^{1/2} L \epsilon_v'^{1/2}, \quad \omega \ll \omega_1, \tag{4.7}$$

which may take on very high values indeed (typically $\gtrsim 10^6$). In this same region the conductivity σ_B varies quadratically with frequency in the form

$$\sigma_B = f L^2 \epsilon_v' \omega^2 / 64\pi^2 \tau, \quad \omega \ll \omega_1. \tag{4.8}$$

As the applied frequency rises to values $\omega \gtrsim \omega_1$ the blocked dielectric constant ϵ_B' begins to fall and goes over to a ω^{-2} frequency dependence

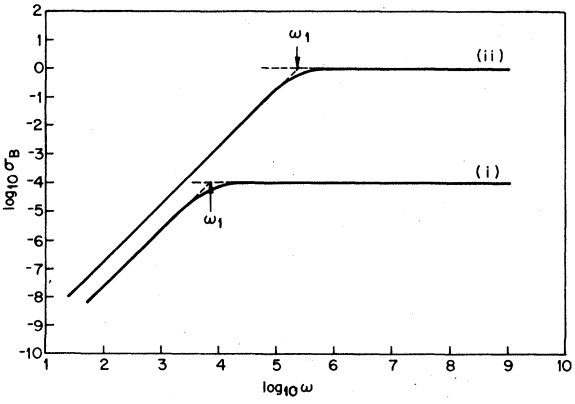

FIG. 3. Blocked conductivity σ_B [in units of $(\Omega\,\text{cm})^{-1}$] computed numerically from Eq. (3.15) as a function of applied angular frequency. Curve (i) corresponds to the material parameters relevant for Fig. 1 and curve (ii) for Fig. 2. Note that 1 $(\Omega\,\text{cm})^{-1}$ is equivalent to 9×10^{11} esu.

$$\epsilon_B' = 32\pi^2\sigma^2 / (f^{1/2} L \epsilon_v'^{1/2} \omega^2), \quad \omega \gg \omega_1, \tag{4.9}$$

while the conductivity settles down to its bulk value (4.4). At still higher frequencies ϵ_B' undergoes a further change and one of two things occurs. If $\epsilon_v' \gg |\epsilon_h'|$, such that the material dielectric constant $\epsilon_v' + \epsilon_h'$ is positive, then ϵ_B' goes smoothly over to its bulk value (4.5) when $\omega > \omega_2$, where

$$\omega_2 = 8\pi\sigma / (2 f^{1/2} L \epsilon_v'^{3/2})^{1/2}, \quad \epsilon_v' \gg |\epsilon_h'|. \tag{4.10}$$

On the other hand, if $\epsilon_v' \ll |\epsilon_h'|$, implying an inductive material response, then the blocked dielectric constant suddenly deviates from (4.9) to go through zero at $\omega = \omega_{ind}$ where

$$\omega_{ind}^2 = \frac{8\pi\sigma}{\tau (f^{1/2} L \epsilon_v'^{1/2} + 4\pi\sigma\tau)}, \quad |\epsilon_h'| \gg \epsilon_v', \tag{4.11}$$

and then becomes negative, finally approaching the bulk material value when $\omega \gtrsim \omega_3$ where

$$\omega_3^2 = 8\pi\sigma / (f^{1/2} L \epsilon_v'^{1/2} \tau), \quad |\epsilon_h'| \gg \epsilon_v'. \tag{4.12}$$

An inductive bulk capacitance implies $4\pi\sigma\tau > \epsilon_v'$ but, since values $f^{1/2} L \gtrsim 10^6$ are typical, one normally has $f^{1/2} L \epsilon_v'^{1/2} \gg 4\pi\sigma\tau$ in which case $\omega_{ind} \approx \omega_3$ such that the switch to induction and saturation at the bulk value follow each other closely in frequency.

All these features can be clearly seen in Figs. 1–3 for which Eq. (4.2) has been solved numerically for both bulk capacitive and bulk inductive situations. Important points to note are that ω_1 and ω_2 (or ω_3) are just the intersection frequencies of the extrapolated low- and high-frequency capacitance-modulus values with the extrapolated linear intermediate frequency section (4.9) on a log-log plot. In addition, from (4.6) and (4.12) we find the very simple ratio

$$\omega_3^2 / \omega_1 = 1/\tau, \tag{4.13}$$

a relationship that provides a rather direct measure of the characteristic relaxation time τ of the itinerant ions. Finally, from (4.6) and (4.10) we note the relation

$$\omega_2^2 / \omega_1^2 = f^{1/2} L / 2 \epsilon_v'^{1/2}. \tag{4.14}$$

Since, as a function of increasing temperature, ionically conducting materials will, in general, progress from a bulk capacitative response to an inductive one, a quite detailed analysis is available via the set of equations set out above. Thus, at lower temperatures, a direct measurement of ϵ_v' and f is possible leading to an estimate for the hopping ion density p_0. Then, since the temperature dependence of f is known from (2.12), measurements in the inductive response regime can provide for a separate determination of ϵ_v' and σ as functions of temperature and finally of the temperature dependence of τ and

$$\epsilon_h' = -4\pi\sigma\tau\,. \tag{4.15}$$

Most importantly, if accurate experiments were available as function of frequency, temperature, and possibly electrode separation L, it would now be possible to determine unambiguously whether observed anomalies in ϵ_B' (such as, for example, are found in amorphous $LiNbO_3$)[7] are intrinsic material anomalies rather than blocking effects and, if so, whether they originate from the vibrational or hopping mechanisms.

V. APPLICATIONS

A full analysis in terms of the above interfacial polarization results requires ideally experimentation as a function of frequency, temperature, and electrode separation L. Nowhere have we found in the literature complete data in this respect for any ionic conductor. Nevertheless, limited data are available for several materials, enough to examine briefly a few of the broader consequences of the equations, and we set out below a few findings for the three ionic conductors Ag_4RbI_5, Li_4SiO_4, and vitreous $LiNbO_3$.

A. Ag_4RbI_5

Armstrong and Taylor[2] have measured room-temperature dielectric response ϵ_B' and σ_B for this conductor between frequencies of 1 and 10^8 Hz, using Pt electrodes for blocking the itinerant silver cations. Their capacitance measurements (Fig. 3D of Ref. 2) bear a striking resemblance to Fig. 2 of this paper, exhibiting an excellent ω^{-2} variance between ω_1 and ω_3, and undergoing a sudden inductive transition at $\omega_{ind} \approx \omega_3 \approx 9\times10^5$ Hz. Material dispersion, following Eq. (4.1), is observed above 10 MHz enabling a direct (i.e., nonblocking) evaluation of τ to be obtained directly from the data. Armstrong and Taylor find the value $\tau \approx 7\times10^{-9}$ sec. The resistance measurement is frequency independent with $\sigma_B = \sigma \approx 0.23\ (\Omega\ \mathrm{cm})^{-1}$ below material dispersion until blocking takes over at ω_1. Below ω_1 the measured conductivity σ_B varies closer to ω^1 than the ω^2 form of (4.8), and this may indicate the breakdown of the theory for surface layer dominated resistive response alluded to earlier.

From the experimental capacitance observation $\epsilon_B'(\omega \to 0) \approx 6\times10^7$ we estimate, from Eq. (4.7), that

$$f^{1/2} L \epsilon_v'^{1/2} \approx 1.2\times10^8\,, \tag{5.1}$$

and hence, from (4.6), (4.10) and (4.11), predict values

$$\log_{10}(\omega_1) \approx 3.8\,, \quad \log_{10}(\omega_{ind}) \approx \log_{10}(\omega_3) \approx 5.6\,, \tag{5.2}$$

with all frequencies in Hz, assuming $|\epsilon_h'| \approx 2\times10^4$ to be large compared with ϵ_v'. Experimentally, from the capacitance scan of Fig. 3D of Ref. 2, we have $\log_{10}(\omega_1) \approx 3.6$, and $\log_{10}(\omega_{ind}) \approx \log_{10}(\omega_3) \approx 5.9$, in good agreement with theory. Values for ϵ_v' and p_0 cannot be deduced from the room-temperature data alone.

B. Li_4SiO_4

Hodge *et al.*[3] have measured ϵ_B' and σ_B for Li_4SiO_4 as a function of frequency between a few hundred cycles and a few megacycles at several different temperatures (using gold electrodes to block the itinerant Li^+). Unfortunately, however, none of the frequency scans covers a full range $\omega \ll \omega_1$ to $\omega \gg \omega_2, \omega_3$, so that again only a partial analysis is possible. At the lower temperatures, for which conductivity is small [$10^{-7}(\Omega\ \mathrm{cm})^{-1}$ at 153°C], the material dielectric constant ϵ_v' is directly measureable above ω_2 and is of order 10. However, conductivity rises exponentially with temperature and inductive transitions are seen on the frequency scans at 488 and 623°C. The 623°C scan is most complete, although full blocking is never attained and Hodge *et al.*[3] do not give the full details of the inductive response magnitude. Nevertheless, at 623°C we observe directly from the data the experimental values

$$\begin{aligned} &\sigma \approx 5\times10^{-2}\ (\Omega\ \mathrm{cm})^{-1}\,, \quad \epsilon_B'(\omega \to 0) \approx 10^8\,, \\ &\omega_{ind} \approx 8\times10^4\ \mathrm{Hz}\,, \quad \omega_1 \approx 10^2 \to 10^3\ \mathrm{Hz}\,. \end{aligned} \tag{5.3}$$

From the appropriate equations of Sec. III we evaluate

$$\begin{aligned} &f^{1/2} L \epsilon_v'^{1/2} \approx 2\times10^8\,, \quad \omega_1 \approx 900\ \mathrm{Hz}\,, \\ &\tau \approx 2\times10^{-8}\ \mathrm{sec}\,, \quad |\epsilon_h'| \approx 10^4\,. \end{aligned} \tag{5.4}$$

The estimate for relaxation time τ (deduced from the observed ω_{ind}) is several times larger than that for Ag_4RbI_5 above. The larger value is supported by the conductance dispersion which is observed at frequencies above ω_{ind} and which suggests a value $\tau \approx 5\times10^{-8}$ sec. However, Hodge *et al.* also observe the inductive transition at 488°C, where $\sigma = \sigma(488) \approx 3\times10^{-3}\ (\Omega\ \mathrm{cm})^{-1}$ and find it at a frequency $\omega_{ind}(488)$ which is slightly greater than $\omega_{ind}(623)$. Theoretically, as long as $|\epsilon_h'| \gg \epsilon_v'$, we expect from (4.11) that

$$\frac{\omega_{ind}(488)}{\omega_{ind}(623)} \approx \frac{\sigma^{1/2}(488)}{\sigma^{1/2}(623)} \approx 0.25\,, \tag{5.5}$$

if ϵ_v' and τ are not temperature dependent [in which case $\epsilon_h'(488) \approx 700$]. For an oxygen tetrahedral network we do not anticipate a marked temperature dependence for dielectric constant ϵ_v', and the data therefore suggest that the relaxation time τ may well be a strongly increasing function of tempera-

ture (or perhaps more significantly of conductivity). The fact that the conductivity dispersion above ω_{ind} is not seen at 488°C in the available frequency range (to 3×10^6 Hz) as it is at 623°C is a possible confirmation of this effect.

C. Vitreous $LiNbO_3$

Vitreous $LiNbO_3$ has been prepared in the form of wafer samples and has a limiting low-temperature dielectric constant of $\epsilon_B' = \epsilon_v' \approx 25$.[7,12,13] Experiments have been performed with both face electrodes ($L = L_f \approx 1.5$ μm) and edge electrodes ($L = L_e \approx 7.5$ μm) the different configurations giving qualitatively different measurements for ϵ_B' at high temperatures. At an applied frequency of 1 kHz, using blocking gold facial electrodes, the T dependence of ϵ_B' was reported in Ref. 7. This in-phase response rises to ≈60 at room temperature[12] and then very rapidly to a peak[7] $\epsilon_B' \approx 4\times10^5$ at 650°K followed by a second peak of roughly equal magnitude at the crystallization temperature T_{cryst} ≈770°K. It has been conjectured[7] that the lower peak may represent a diffuse dielectric instability (i.e., large values of ϵ_v').

The situation is complicated, however, by the fact that vitreous $LiNbO_3$ becomes an increasingly good ionic conductor as T rises with conductivity (above ω_1) about 5×10^{-6} $(\Omega\ \text{cm})^{-1}$ at room temperature and close to 10^{-3} $(\Omega\ \text{cm})^{-1}$ at 500°K.[13] Unfortunately, conductivity measurements in the peaked ϵ_B' region are not yet available. However, it is clear that a quantitative description of these peaks must take into account the conductivity and the possibility of a development of interfacial polarization.

At room temperature, with edge electrodes, the value of ω_1 (from resistivity data[13]) is ≈3 Hz. If $\epsilon_B' \approx \epsilon_v'$ at room temperature (see below) with a value 60, then we calculate from (4.6), (4.7), and (4.10) the theoretical estimates

$$f^{1/2}L_e \approx 8\times10^5, \quad \omega_2 \approx 660\ \text{Hz}, \quad \epsilon_B'(\omega\to0) \approx 3\times10^6, \tag{5.6}$$

at this temperature, assuming $|\epsilon_h'| \ll \epsilon_v'$ (which corresponds to $\tau \ll 10^{-6}$ sec). The value $\omega_2 \approx 660$ Hz implies that the greater part of the increase in observed dielectric constant between 0 and 300°K is indeed a true material effect and not due to interfacial polarization. From (5.6) and (2.12) we now find a mobile ion density

$$p_0 \approx 2\times10^{20}\ \text{cm}^{-3}, \tag{5.7}$$

which implies that only about 1% of the available Li ions are actually participating in the macroscopic ionic motion at these temperatures.

As T rises, the frequencies ω_1 and ω_2 (being dominated by σ) increase rapidly so that at higher temperatures all data taken at 1 kHz (or below) are undoubtedly influenced strongly by interfacial polarization. Though a detailed analysis of the high-temperature peaks in ϵ_B' must await further conductivity measurements, one observation from Ref. 7 is highly informative. It is that the change from face to edge electrodes increases the T_{cryst} peak by a factor of 5 (to ~2×10^6) while leaving the 650°K peak unchanged or decreased (it becomes a shoulder on the higher T peak). This implies that ϵ_B' at 770°K is fully blocked [with a magnitude $\propto L$ from (4.7)]. It follows from the room-temperature data (5.6) that $\epsilon_B'(\omega\to0)$ at T_{cryst} is close to its value at 300°K and that accordingly the value of ϵ_v' at T_{cryst} is not significantly greater than 60. At the lower peak, however, ϵ_B' is obviously not fully blocked. A large value of ϵ_v' in this region, which would decrease ω_1 of (4.6), would be in accord with this observation and an explanation in terms of a diffuse dielectric instability near 650°K remains an intriguing possibility.

---

[1] M. E. Lines, preceding paper, Phys. Rev. B 19, 1183 (1979).
[2] R. D. Armstrong and K. Taylor, J. Electroanal. Chem. 63, 9 (1975).
[3] I. M. Hodge, M. D. Ingram, and A. R. West, J. Am. Ceram. Soc. 59, 360 (1976).
[4] K. Funke and A. Jost, Ber. Bunsenges. Phys. Chem. 75, 436 (1971).
[5] K. Funke and R. Hackenbury, Ber. Bunsenges. Phys. Chem. 76, 885 (1972).
[6] B. A. Huberman and J. B. Bryce, Solid State Commun. 25, 759 (1978).
[7] A. M. Glass, M. E. Lines, K. Nassau, and J. W. Shiever, Appl. Phys. Lett. 31, 249 (1977).
[8] M. E. Lines, Phys. Rev. B 17, 1984 (1978).
[9] G. Jaffe, Phys. Rev. 85, 354 (1952).
[10] J. R. MacDonald, Phys. Rev. 92, 4 (1953).
[11] In this equation, ϵ_v is the dielectric function of the material in the absence of mobility. It should therefore be understood in this and all subsequent equations as including *all* nonconducting (and vacuum) contributions to dielectric response.
[12] A. M. Glass (private communication).
[13] A. M. Glass, K. Nassau, and T. J. Negran, J. Appl. Phys. 49, 4808 (1978).